

VESPA

Vaso per Esperimenti Su Plasmi ed Altro

Andrea Grossutti, mat. 1237344
Alessandro Lovo, mat. 1236048
Leonardo Zampieri, mat. 1237351

December 25, 2019

1 Aims

Study the *Vespa* experimental apparatus, and in particular:

- Model the vacuum system behavior, finding the characteristic parameters;
- Obtain the current-voltage and the current-temperature characteristics curves of the filament;
- Draw the voltage-current characteristics curves of the gas discharge, enhancing their behavior as varying pressure;
- Find the Paschen curve, both in DC and RF condition;
- Measurement of plasma parameters through a Langmuir probe, both in stationary conditions and via ionic-sonic wave propagation.

2 Vacuum system

The vacuum inside the VESPA vessel (a cylindrical vessel, with a length of $\sim 80\text{cm}$ and a radius of $\sim 20\text{cm}$: $V \sim 0.1\text{m}^3$) is obtained and kept thanks to a rotary pump and a turbomolecular pump. The vessel is not perfectly isolated and some small leaks affect the vacuum keeping. To study this phenomena, the vessel has been taken to a low pressure ($\sim 6 \cdot 10^{-5}\text{mbar}$) and all the valves around have been closed. Isolating the chamber from the pumping system one can measure (thanks to a ionization pressure gauge) the pressure in the vessel as function of time. Effects as leaks and degasing contribute to an inflow in the chamber $F_0(p)$ that in principle could depend on the pressure. Assuming instead F_0 constant, its value can be estimated through a linear fit on the data: $P = a + b \cdot t$, $F_0 = V \cdot b$.

Considering the reaction time, the slowness of the ionization gauge in stabilizing and the pressure oscillations, the errors are estimated as 5% on the pressure and a 0.5s error on the time.

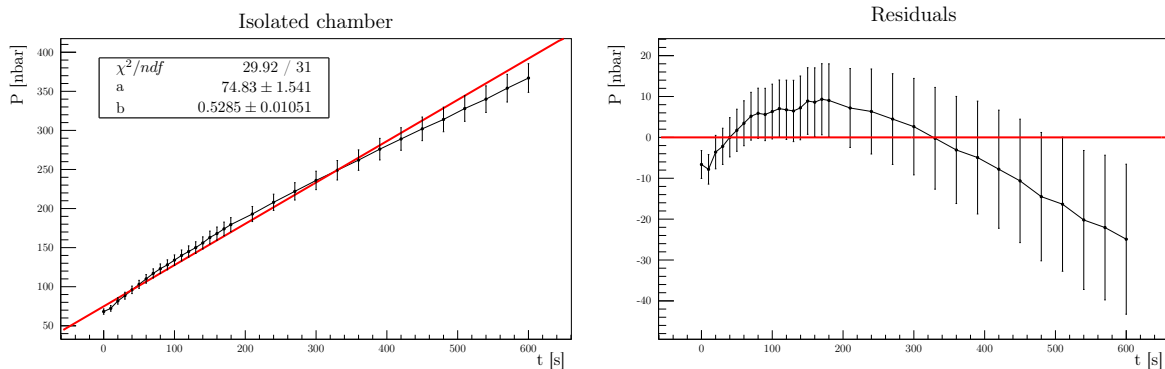


Figure 1: Presure increasing in the chamber

As can be seen from fig 1 there is an evident trend in the residuals, proving that F_0 cannot be assumed constant throughout all the explored range of pressures. A simple way to correct this is to

consider a low pressure regime and a high pressure one: the limit has been put where the trend in the residuals inverts, i.e. around 200nPa.

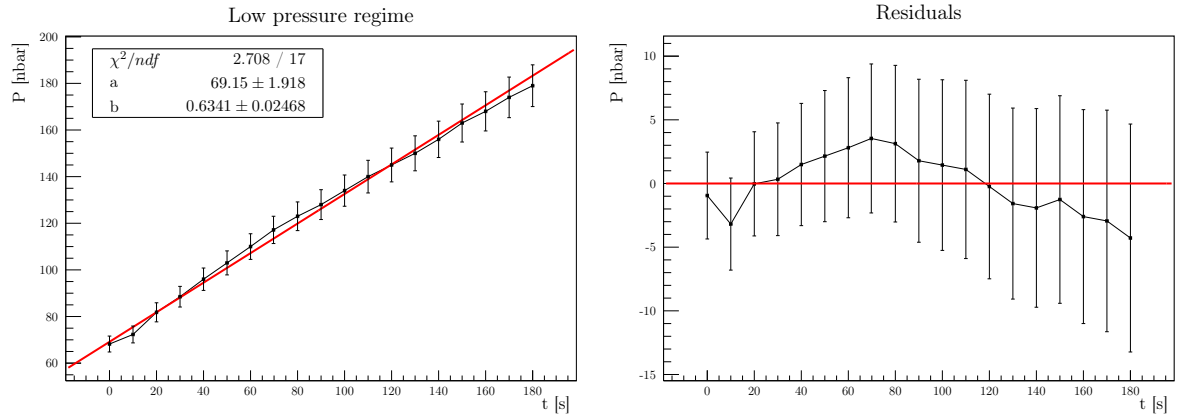


Figure 2: Low pressure regime

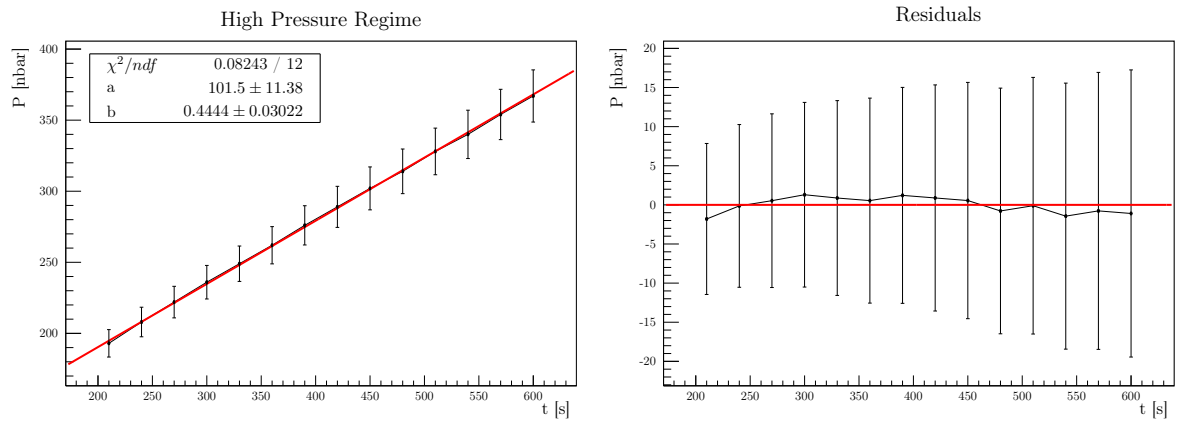


Figure 3: High pressure regime

Secondo me è un po' un casino, un po' tutto stretto. Proporrei invece al posto delle figure 3 e 2 la figura seguente:

Low and High pressure regimes

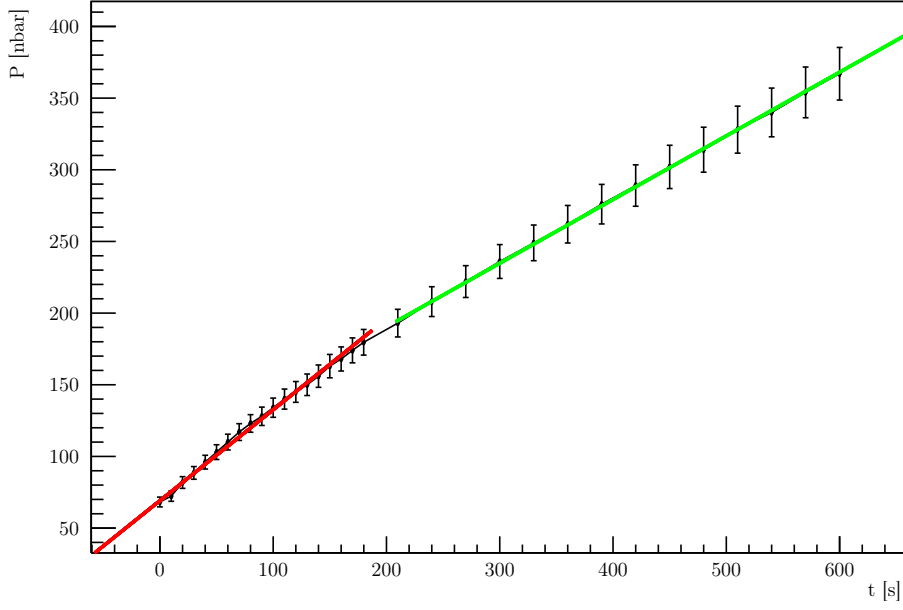


Figure 4: Fits in the two regimes.

Splitting the high pressure area and the low pressure area, performing two different fits and assuming a 5% error on the volume, the inflow can be estimated as:

$$F_0^{\text{low}} = (6.4 \pm 0.4) \cdot 10^{-6} \text{Pa m}^3/\text{s}, \quad F_0^{\text{high}} = (4.5 \pm 0.4) \cdot 10^{-6} \text{Pa m}^3/\text{s}$$

Subsequently, the valve has been opened connecting the chamber to the pumping system. An exponential decay of the pressure is expected: $P(t) = (P_i - P_0) \exp(-t/\tau) + P_0$, where P_i is the starting pressure and P_0 the asymptotic pressure.

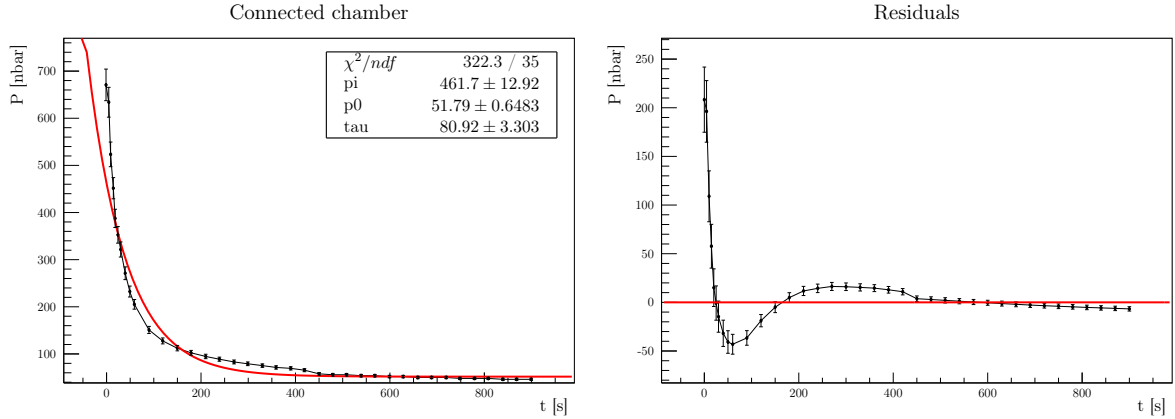


Figure 5: Pressure decreasing in the chamber

As can be seen from fig 5, similarly as what seen before, the result are not acceptable and as before two regimes can be distinguished. For coherence the same limit as before has been used.

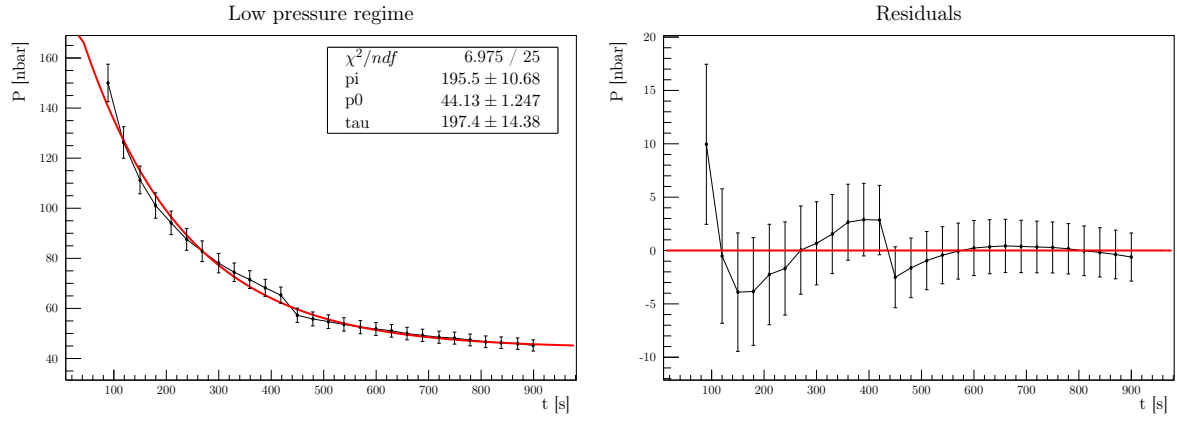


Figure 6: Low pressure regime

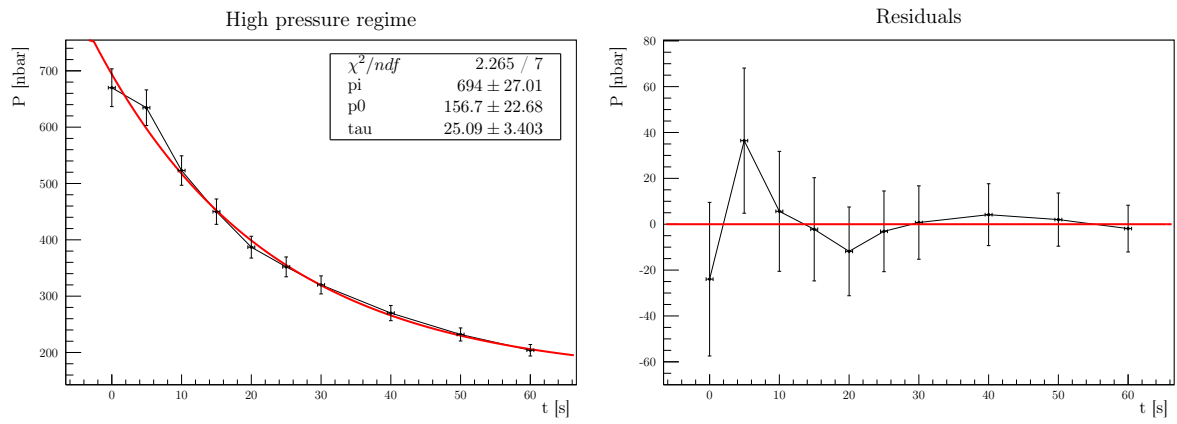


Figure 7: High pressure regime

Facendo un grafico in scala logaritmica, sembra invece che ci siano tre regimi! Vedere figura seguente

Different regimes in chamber emptying

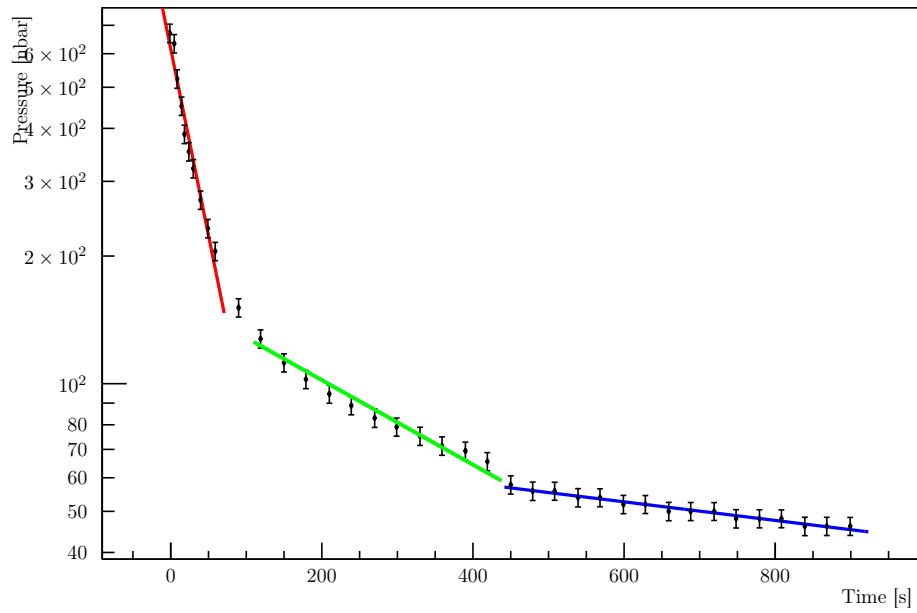


Figure 8: Fits in different regimes.

Performing two different exponential fits there are still trends in the residuals, but now the result

is acceptable. From the values of τ and P_0 the effective pumping speed S_e , the inflow F_0 and, given the nominal value of the pumping speed $S = 331/\text{s}$, the conductance of the chamber-pump connection C can be estimated.

regime	$S_e = V/\tau$ [l/s]	$F_0 = P_0 \cdot S_e$ [Pa m ³ /s]	$C = 1/(1/S_e - 1/S)$ [l/s]
low pressure	0.51 ± 0.04	$(2.2 \pm 0.2) \cdot 10^{-6}$	0.52 ± 0.05
high pressure	4.0 ± 0.6	$(2 \pm 1) \cdot 10^{-5}$	4.6 ± 0.7

Table 1: Vacuum parameters

In the low pressure regime the two estimates of F_0 are not compatible but still comparable, on the other hand at high pressure the two estimates differ by an order of magnitude. By comparing the nominal value of the pumping speed with S_e one can deduce that most of the pump potential is wasted by a very low conductance connection.

3 Voltage-Current characteristic of the filament

The filament inside the vessel is a tungsten filament with diameter $2r \sim 0.25\text{mm}$ and length $L \sim 10\text{cm}$. Combining Ohm law and emissivity rules, a theoretical characteristic curve can be obtained:

$$V = \frac{A^{10/7} L}{\pi^{13/7} r^{23/7} (2\epsilon\alpha)^{3/7}} \cdot I^{13/7}$$

where ϵ is the effective emissivity, α the StefanBoltzmann constant and A a the resistivity proportional constant, such that the resistivity ρ can be expressed as function of the temperature T as

$$\rho(T) = AT^{6/5}$$

Pumping the vessel to a low pressure (~ 2), the voltage-current characteristic curve of the filament has been measured, producing the following data:

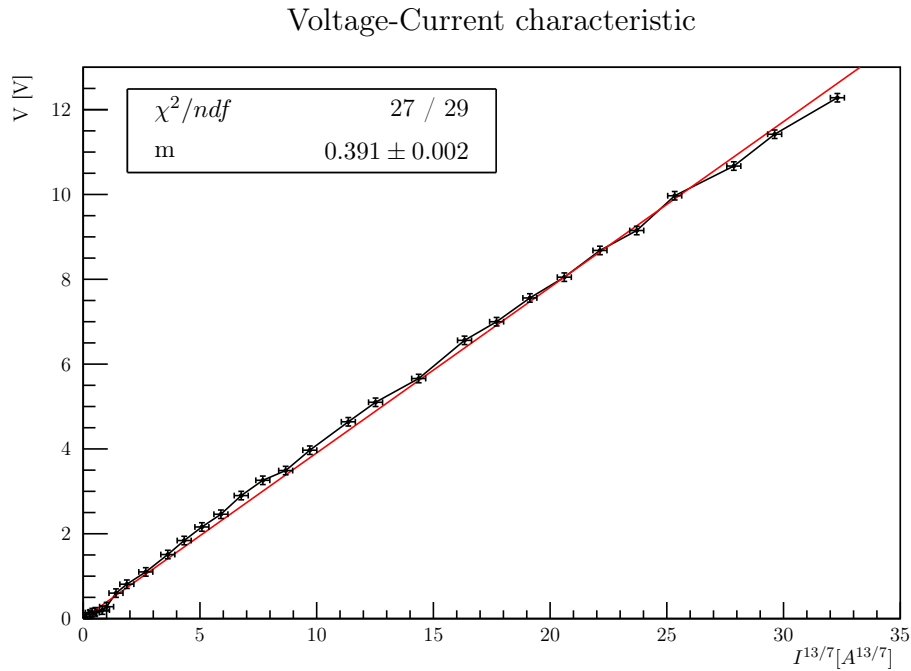


Figure 9: Voltage-Current characteristic for a filament; errors has been chosen as $0.3A^{13/7}$ and $0.1V$, due to the low sensibility of the measure system.

Fitting the data with a $V \propto I^{13/7}$, the following parameters are found:

$$V = mI^{13/7} \quad (1)$$

$$m = (0.391 \pm 0.002)V \cdot A^{-13/7} \quad (2)$$

which lead to a value of

$$\epsilon \sim 0.2$$

The χ^2 confirm the meaningfulness of the fit; moreover, the effective emissivity has a value similar to the typical ones (0.3).

Finally, the estimated filament temperature as a function of the driven current can be found:

$$T = \underbrace{\frac{A^{5/14}}{\pi^{5/7} r^{15/14} (2\epsilon\alpha)^{5/14}}}_k \cdot I^{5/7} \quad \text{with } k \sim 811 \text{K} \cdot A^{-5/7}$$

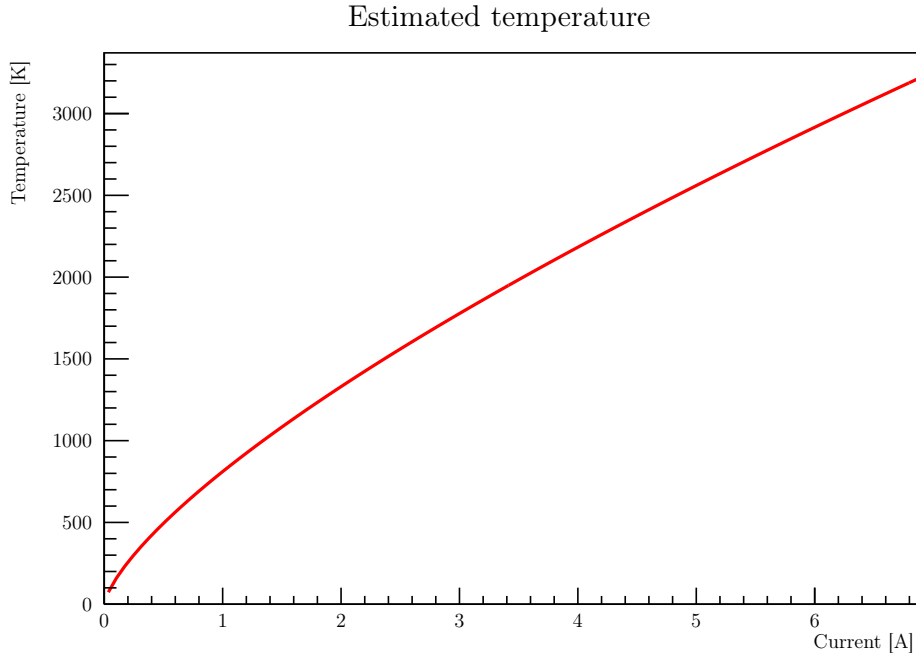


Figure 10: Projection of the filament temperature as function of the current

4 V-I characteristics of the discharge & DC Paschen curve

By polarizing the filament with respect to the whole vessel (grounded) a discharge in the plasma can be achieved. By measuring the polarization voltage on the power supply (0.1V estimated error) and the plasma current via the voltage across a resistor $R_{\text{shunt}} = (1.00 \pm 0.03)\Omega$, the discharge characteristic curve can be studied. In particular the breakdown is clearly visible.

4.1 Varying I_f

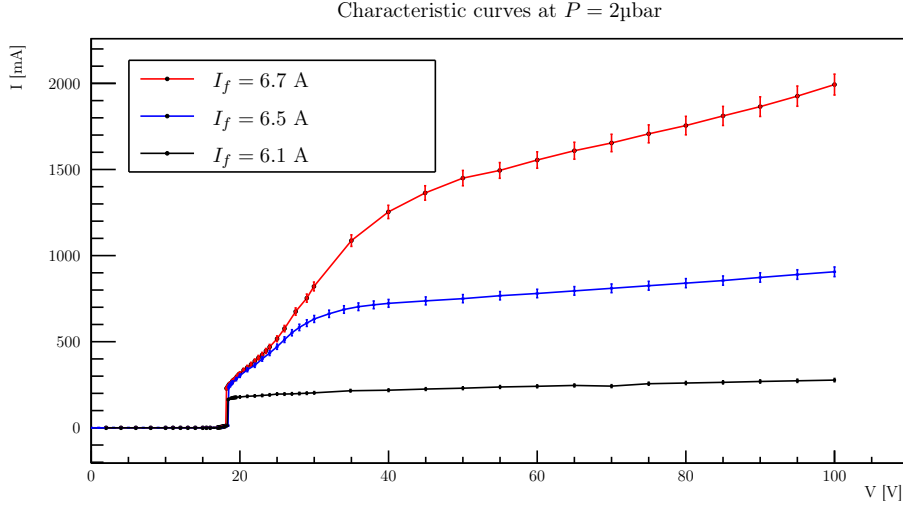


Figure 11: V-I characteristics of the discharge at constant pressure P , varying the filament current I_f . The breakdown is clearly visible around ~ 18 V.

As can be seen from fig 11, variations on filament current doesn't affect breakdown voltage, but changes the behavior of the plasma once it is ignited.

The current emitted by the filament into the plasma can be modeled by Richardson law:

$$I = \Sigma A T^2 \exp\left(-\frac{e\Phi}{k_B T}\right)$$

where for our tungsten filament $A = 7 \cdot 10^5 \text{ A/m}^2 \text{ K}^2$, $\Phi = 4.55 \text{ V}$ and $\Sigma = 2\pi r L \sim 80 \text{ mm}^2$ is the surface area of the filament. By using the previous found relation between the temperature and the filament current $T = k \cdot I_f^{5/7}$, and assuming that the plasma current is the whole current emitted by the filament, an expression for the current can be obtained:

$$I = J I_f^{10/7} \exp\left(-Q I_f^{-5/7}\right) \quad \text{where:} \quad J = \Sigma A k^2 \sim 3.6 \cdot 10^7 \text{ A}^{-3/7} \quad Q = \frac{e\Phi}{k_B k} \sim 65 \text{ A}^{5/7}$$

Richardson law predicts no dependence of the plasma current on the polarization voltage V , so a first comparison between the predicted plasma current and the experimental one is to use for the latter the value at $V = 60 \text{ V}$: value at which the plasma has been ignited but the electric field is not strong enough to induce a high multiplication of electrons.

I_f [A]	I^{exp} [A]	I^{Rich} [A]	$I^{\text{Rich}}/I^{\text{exp}}$
6.1	0.2	8	34
6.5	0.8	20	25
6.7	1.6	30	19

Table 2: Experimental plasma current at $V = 60 \text{ V}$ and prediction from Richardson law (since the discrepancies between theoretical and experimental values are very high only approximate values are shown).

Continuano a non convincermi questi valori un po' così. Ma se non troviamo nessuna alternativa ok.

As can be seen from tab 2 the prediction and the data differ by a factor ~ 25 , that is almost the same for every value of the filament current, suggesting that the main error is either in the estimate of coefficient J or in the assumption that the current emitted by the filament is the plasma current. The latter seems more reasonable since the plasma current varies with V and can be explained by the predominance of electron absorption in the plasma at low V and electron multiplication at high V .

In this case the error in the prediction of the current could be used as an estimate of the percentage of absorbed electrons: $\sim 96\%$.

On the other hand during data acquisition it has been observed that the voltage across the filament V_f increases with V , meaning that the resistivity of the filament becomes greater. This means either that the resistivity does not depend only on the temperature of the filament, or that the temperature does not depend only on I_f .

Da dove è uscito 'sto numero?

4.2 Varying P

By studying instead the V-I characteristics varying the Argon pressure one obtains the results in fig 12. If one ignores the weird behavior of the $P = 8 \mu\text{bar}$ curve at high V , it is visible that the main influence of the pressure on the curve is the value of the breakdown voltage, effect that can be better understood building the experimental Paschen curve (fig 13).

Sono due punti palesemente sbagliati, reiettiamoli e basta secondo me

Come l'abbiamo costruita?

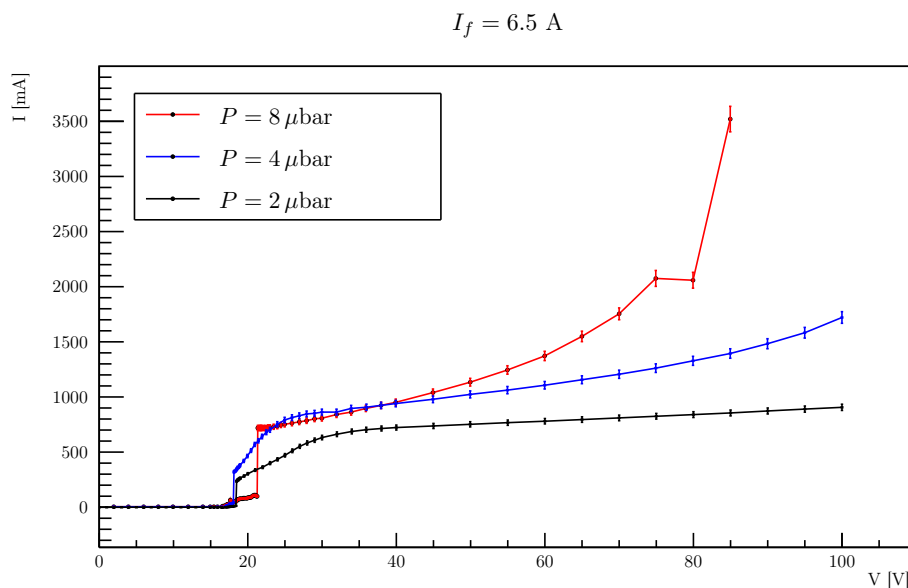


Figure 12: V-I characteristics of the discharge at constant filament current I_f , varying the pressure P

DC Paschen curve

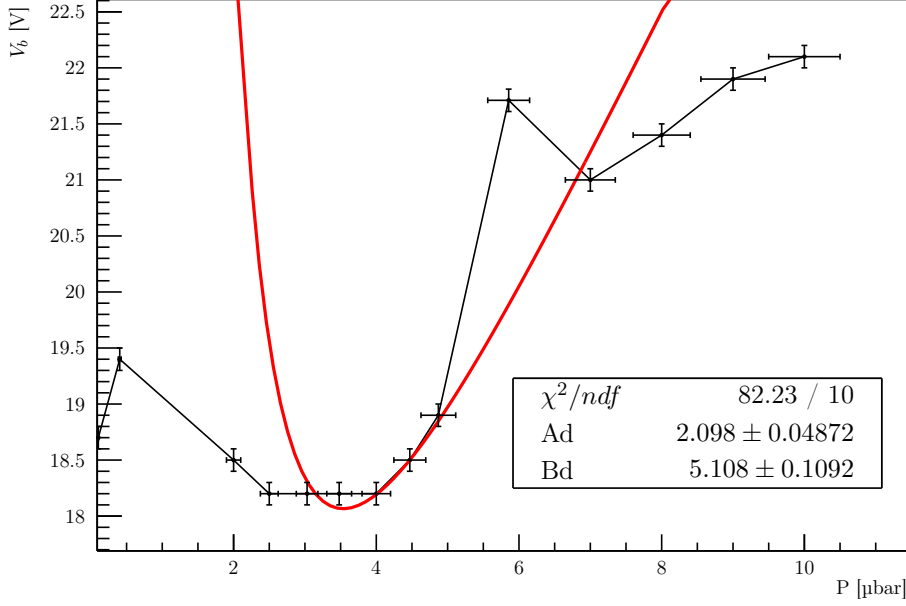


Figure 13: Experimental Paschen curve: breakdown voltage vs P

No amici, questo fit è inguardabile, non prende nemmeno bene il minimo, direi di ammazzarlo

The theoretical formula of the Paschen curve is

$$V_b = \frac{Bpd}{\log(Apd) - C} \quad (3)$$

where d is the distance between the electrodes and for Argon $A = 8.63\text{m}^{-1}\text{Pa}^{-1}$, $B = 132.0\text{Vm}^{-1}\text{Pa}^{-1}$ and $C = 1.004$. By keeping C fixed* at the theoretical value and varying A and B it is possible to perform a fit on the data (fig 13). A way to compare the results of the fit with the theoretical ones is to take consider the ratio A/B :

$$\left(\frac{A}{B}\right)_{\text{experimental}} = \left(\frac{Ad}{Bd}\right) = (0.41 \pm 0.01)\text{V}^{-1} \quad \left(\frac{A}{B}\right)_{\text{theoretical}} \sim 0.07\text{V}^{-1}$$

Dai, non mi serve un conto così complicato per vedere che la curva non fitta.

As can be seen the experimental results do not agree with the theory both in the sense that the fit with the theoretical curve has a very high χ^2 and in the sense that the fitting parameters are incompatible with the expected theoretical values.

Another way to see this incompatibility is that from fig 13 it is clear that Paschen's minimum is between 3 and 4 μbar , but this would imply that using the theoretical value for A , $d \sim 2.4 \text{ m}$, that is rather unphysical considering that the whole chamber is only 0.8 m long.

It can then be deduced that this system does not follow the theoretical Paschen's curve.

Non abbiamo dato un risultato, un chiaro valore per questo minimo

5 Paschen curve in radiofrequency condition

Inside VESPA a magnetic antenna is provided, which allow to induce a plasma through radiofrequency waves that, coupling with gas electrons, excite them and generate the discharge.

The antenna is powered through a RF generator and a RLC circuit; firstly, the response of the circuit is studied. Keeping fixed the generator power and varying the frequency, through an oscilloscope

*Eventual variations of C can be absorbed into the variation of A , so keeping C fixed is not limiting.

the peak-to-peak amplitude of the wave downstream the circuit is measured. The result is a typical resonance curve (fig. 14).

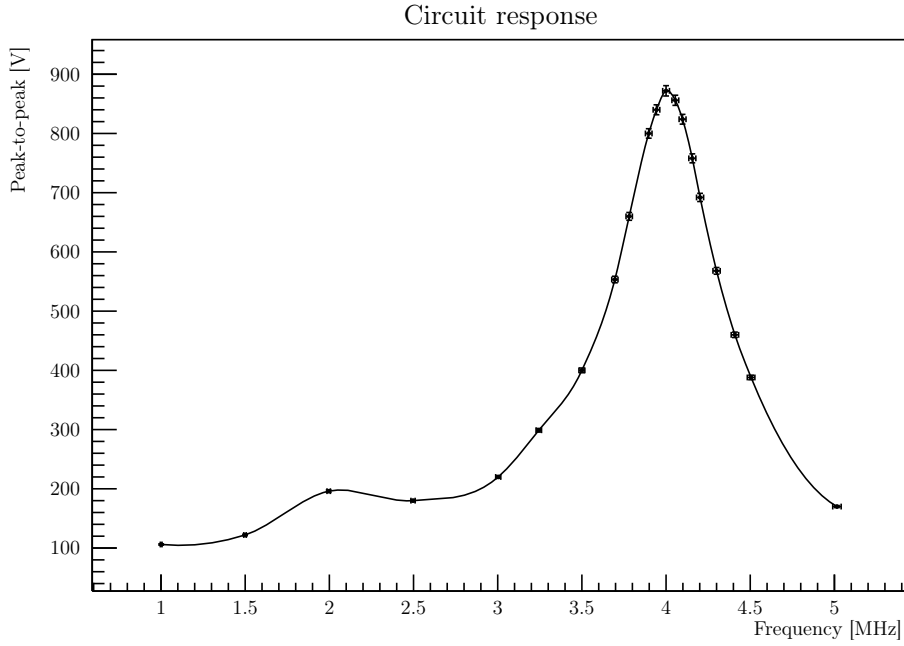


Figure 14: Peak-to-peak amplitude downstream the circuit, varying the wave frequency. From the oscillation in the measurements and the instrumentation sensibility, the errors has been estimated at 5‰ in the frequencies and 1% in voltages.

From the fig. 14 the maximum can be detected: it is around 4MHz. Therefore the operation area is identified in the range 3–4MHz, when the amplitude is high and increasing with the frequency.

Varying the pressure in the vessel, the breakdown voltage trend can be studied. For each pressure, the frequency has been increased until the discharge took place (it's a clearly visible phenomena, so the discrimination has been done visually), and the peak-to-peak voltage in the breakdown point has been measured. The result is the Paschen curve in fig. 15.

Breakdown voltage - RF discharge

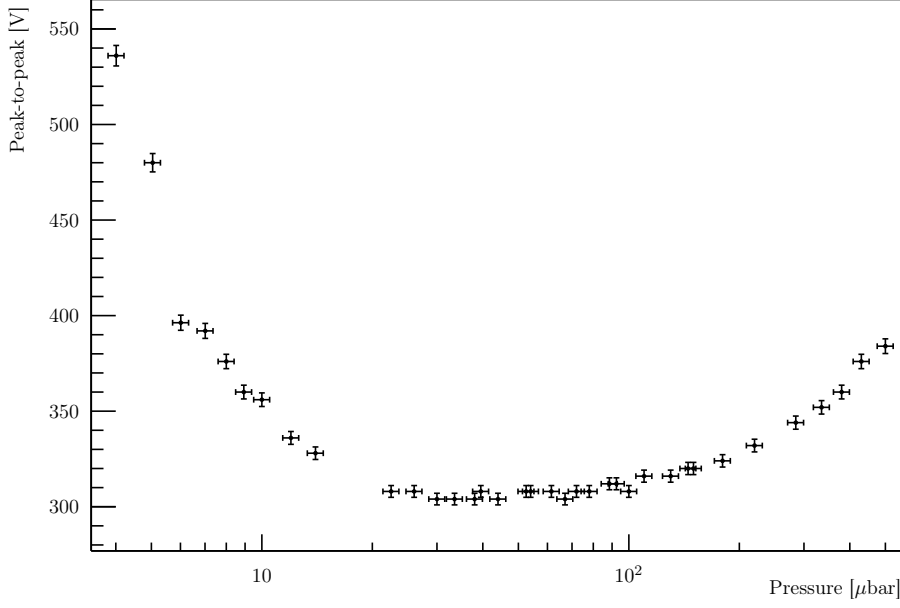


Figure 15: Radiofrequency Paschen curve. From the oscillation in the measurements and the instrumentation sensibility, the errors has been estimated at 5% in the pressures and 1% in voltages.

As can be seen from the plot, the minimum of the Paschen curve in radiofrequency condition is very large: the optimal area can be identified in the range:

$$3-7 \cdot 10^{-5} \text{bar}$$

6 Measurement of plasma parameters

Using a Langmuir probe an estimation of plasma parameters such as density, electron temperature and plasma potential can be obtained, throw electric parameters of the filament of which the probe is composed. The electron current from the probe to the plasma is given by the following formula:[†]

$$I = I_{si} (1 + R(V - V_f)) \left(\exp \left(\frac{e(V - V_f)}{kT_e} \right) - 1 \right)$$

where I_{si} is the *Ion Saturation Current*, V_f is the *Floating Potential*, T_e is the *Electronic Temperature* and R is an additional factor that describes the current-voltage characteristic for $V \ll V_f$. Is important to notice that this formula describes experimental data for $V \lesssim V_f$, while for higher values of V additional terms are required. These terms can be obtained throw fitting procedure. An example of electrical voltage-current characteristics is shown in fig. 16 and 17.

[†]This formula is a different version of the one derivated in D. Desideri and G.Serianni *Four Parameter data fit for Langmuir probes with nonsaturation of ion current*, Rev. Sci. Instrum., 69 (1998), <https://doi.org/10.1063/1.1148942>

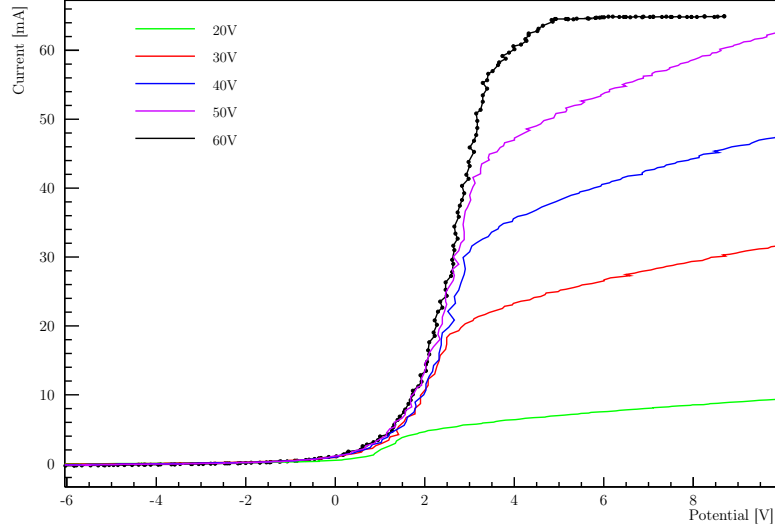


Figure 16: Electrical voltage–current characteristic of the Langmuir probe for a pressure of $2.84\mu\text{bar}$, a filament current of 6.5A and different discharge polarization voltages (as described in legend). In this case the probe is placed in the same side of the filament.

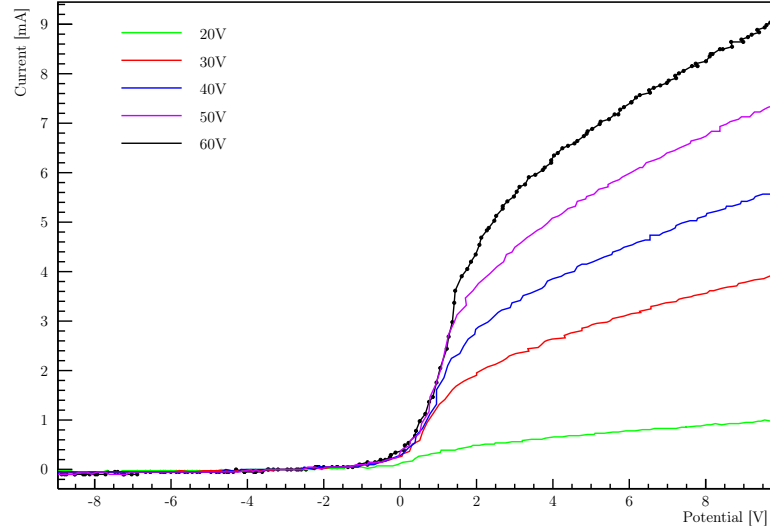


Figure 17: Electrical voltage–current characteristic of the Langmuir probe for a pressure of $2.84\mu\text{bar}$, a filament current of 6.5A and different discharge polarization voltages (as described in legend). In this case the probe is placed in the opposite side to the filament.

Other plasma parameter can be obtained with following formulas:

$$c_s = \left(\frac{e T_e}{m_i} \right)^{1/2}$$

$$n = \frac{2 I_{si}}{e c_s A}$$

$$V_p = V_f + \frac{1}{2} \left(\log \left(\frac{m_i}{2\pi m_e} \right) + 1 \right) T_e$$

where c_s is the *ion sound velocity*, n is the *plasma density*, V_p is the *plasma potential*, m_i is the *ion mass*, A is the *probe area* and e is *electron charge*.

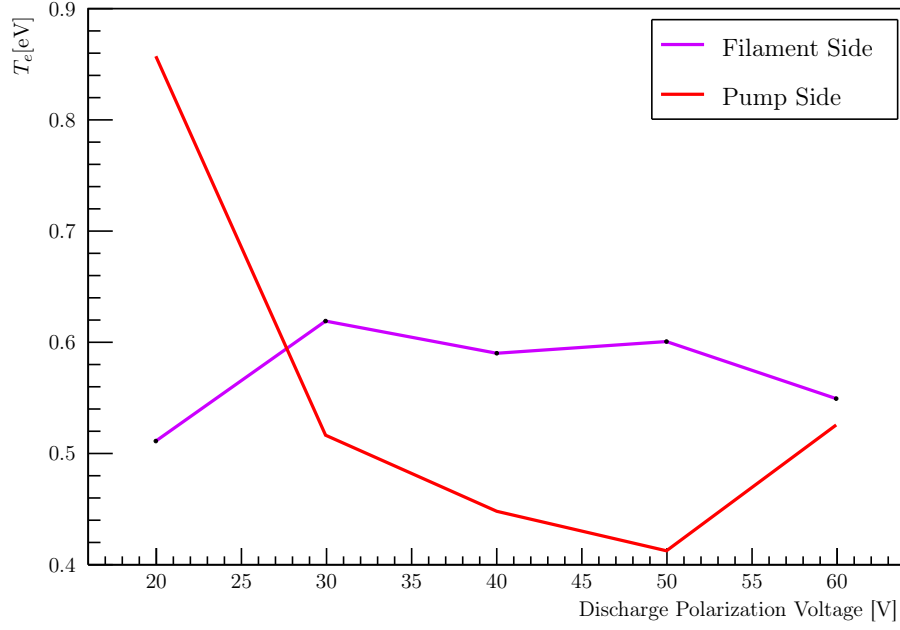


Figure 18: ehi

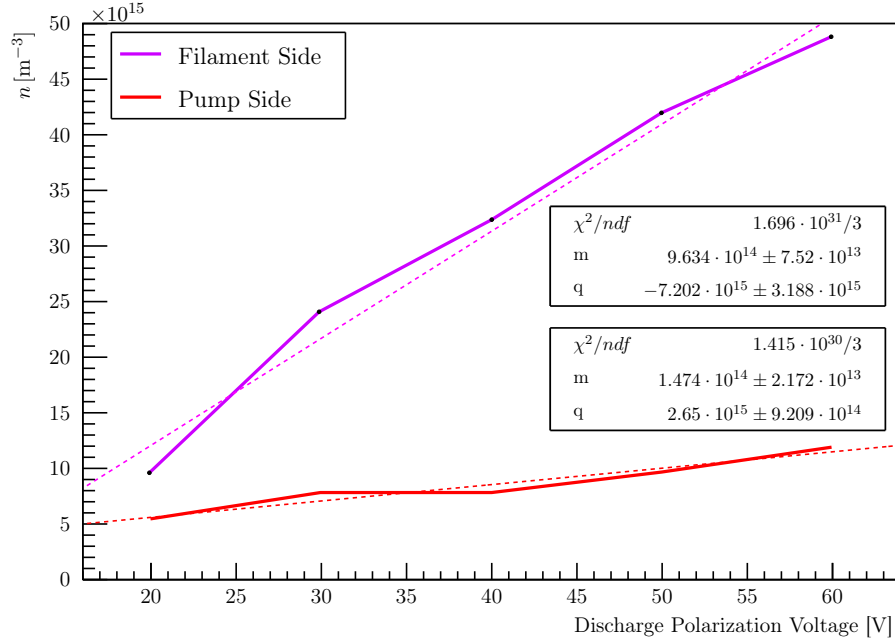


Figure 19: ehi

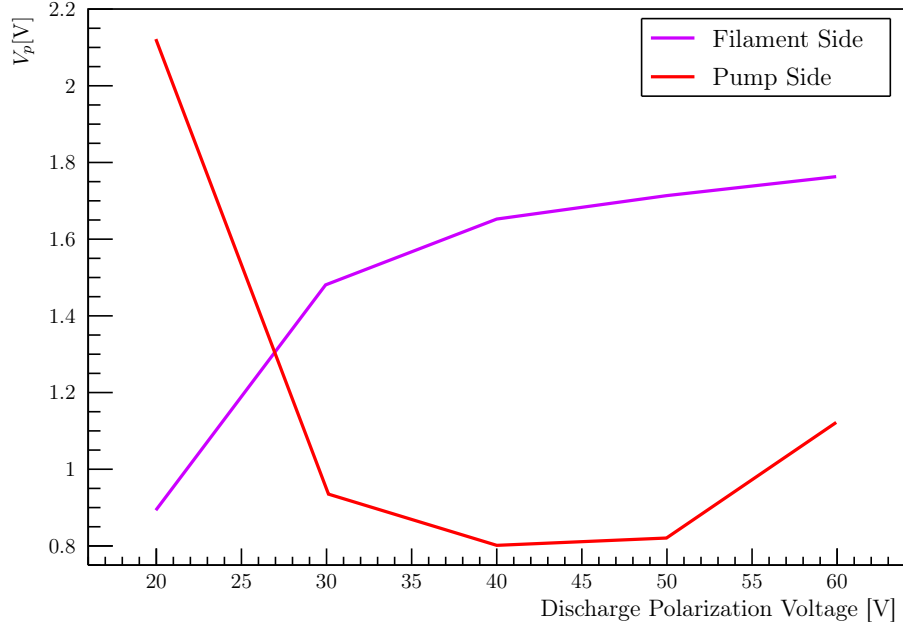


Figure 20: ehi

7 IonicSonic speed

Through the Langmuir probes, some measurements of the ionic-sonic waves propagation can be done. Igniting the plasma with a filament current of 6.5A, the grid has been polarized with a sinusoidal waves (frequency $\sim 20.8\text{kHz}$, $V_{\text{peak-peak}} \sim 50\text{V}$, which also trigger the oscilloscope) and the Langmuir probe has been connected to an oscilloscope. One of the first things noticed is that the plasma distorts the sinusoidal wave: as can be seen from fig. 21, in the output wave the rising time is greater than the lowering time.

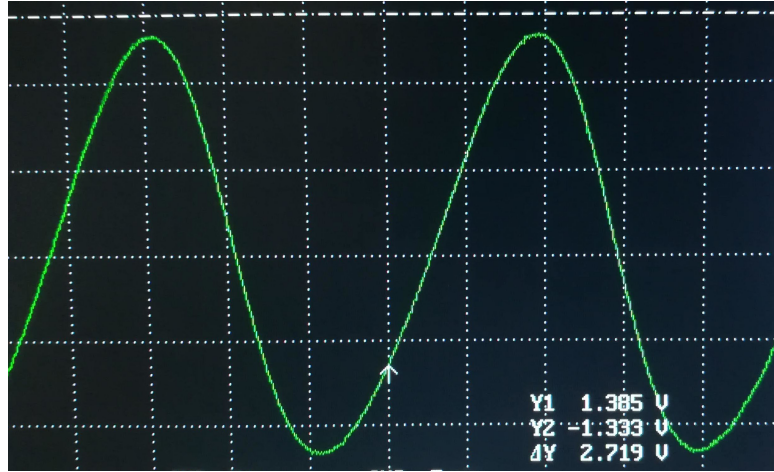


Figure 21: Signal from Langmuir probe: note the distorted sinusoidal wave. Scale: 1 square = $10\mu\text{s} \times 500\text{mV}$

Moving the probe perpendicularly to the grid, the shift of the maximum and minimum of the detected wave has been measured, and thus the speed estimated.

After various tests, searching for the non linear effects (i.e. the distortion of the sinusoidal wave at various position of the probe) to be negligible, the pressure has been set to around $3.26 \cdot 10^{-3}\text{mbar}$ and the polarization voltage to 36.0V. The following measurements has been done:

$\Delta x[\text{mm}]$	$\Delta t_{min}[\mu\text{s}]$	$\Delta t_{max}[\mu\text{s}]$
5.0 ± 0.1	2.0 ± 0.2	5.0 ± 0.2
10.0 ± 0.1	5.0 ± 0.2	7.0 ± 0.2

Table 3: IonicSonic speed: maximum and minimum shifts

$$\begin{aligned}
c_{s,min} &\sim 2.3 \cdot 10^3 \text{ m s}^{-1} \\
c_{s,max} &\sim 1.3 \cdot 10^3 \text{ m s}^{-1} \\
c_s &\sim 1.8 \cdot 10^3 \text{ m s}^{-1}
\end{aligned}$$

In a first approximation,

$$c_s = \sqrt{\frac{k_B T_e}{m_i}}$$

where m_i is the Argon-ion mass ($m_i \sim 6.63 \cdot 10^{-26} \text{ kg}$), which lead to an estimated electron temperature of:

$$T_e \sim 1.3 \text{ eV}$$

Observe that these estimations are very coarse; the used method, the available apparatus and the non-linearity terms doesn't allow a better result.

Compare with predicted one

8 IonicSonic decay

Keeping the same system conditions, the amplitude of the wave as function of the trend has been studied. Moving the probe perpendicularly to the grid and recording the amplitude of the wave, the trend in fig. 22 are found.

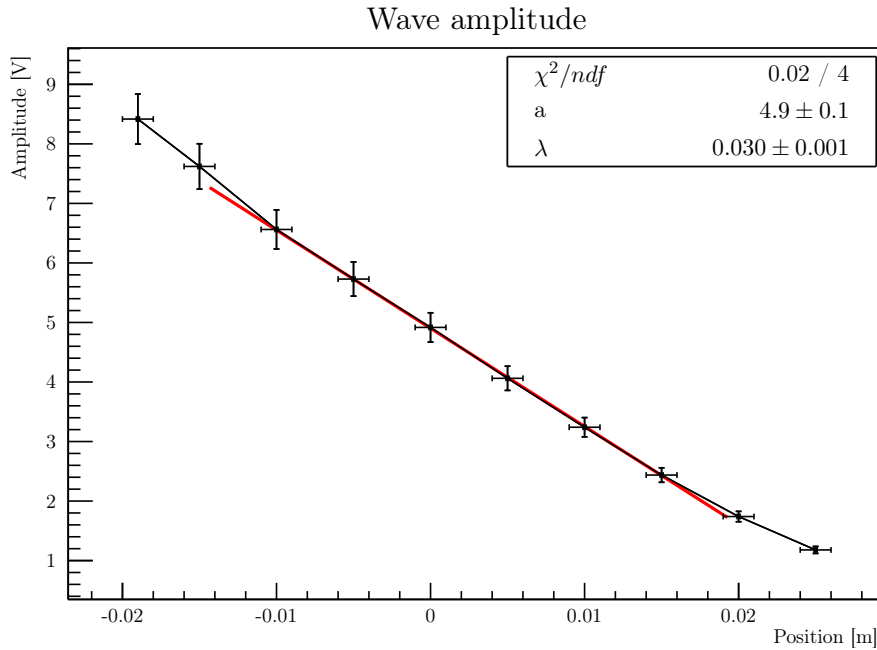


Figure 22: Peak-peak amplitude of the wave as function of the position. The 0 in the x axis has been chosen to be about around the middle of the plot.

From the theory, the amplitude should decay as an exponential. The low range explored doesn't permit a proper exponential fit, thus a first-order approximation around an arbitrary d_0 has been done:

$$Ae^{-d/\lambda} = Ae^{-(d-d_0+d_0)/\lambda} = \underbrace{Ae^{-d_0/\lambda}}_a \left(1 - \frac{d-d_0}{\lambda}\right)$$

Having chosen in the plot the x axis such that it has the 0 around the middle of the fit range, can be assumed $x = d - d_0$. From the fit, the typical length is found:

$$\lambda = (0.030 \pm 0.001)\text{m}$$

This length can be approximated by:

$$\lambda = \frac{2c_s}{v_{te}n_0\sigma_0}$$

being σ_0 the cross section of the electrons with the neutrals ($\sigma_0 \sim 2 \cdot 10^{-20}\text{m}^2$), c_s the previous found ionic-sonic speed and v_{te} the electrons thermic speed ($v_{te} \sim \sqrt{3k_bT_e/m_e} \sim 8.4 \cdot 10^5\text{m s}^{-1}$). This lead to an estimation of the neutral particle density n_0 of:

$$n_0 = 7 \cdot 10^{18}\text{m}^{-3}$$

From the perfect-gas law, we can instead compute (assuming a temperature near to the room one, $\sim 300\text{K}$):

$$p = nk_BT \quad \rightarrow \quad n = \frac{p}{k_BT} \sim 8 \cdot 10^{19}\text{m}^{-3}$$

9 Conclusions

...